ACS ORGANIC & INORGANIC Au
AN OPEN ACCESS JOURNAL OF THE AMERICAN CHEMICAL SOCIETY

pubs.acs.org/orginorgau
Article

Nitrogen-Enriched Biguanidine-Functionalized Cobalt Ferrite Nanoparticles as a Heterogeneous Base Catalyst for Knoevenagel Condensation under Solvent-Free Conditions

Anupam Mishra,[$] Priyanka Yadav,[$] and Satish K. Awasthi*

Cite This: ACS Org. Inorg. Au 2023, 3, 254−265
Read Online

ACCESS | Metrics & More | Article Recommendations | Supporting Information

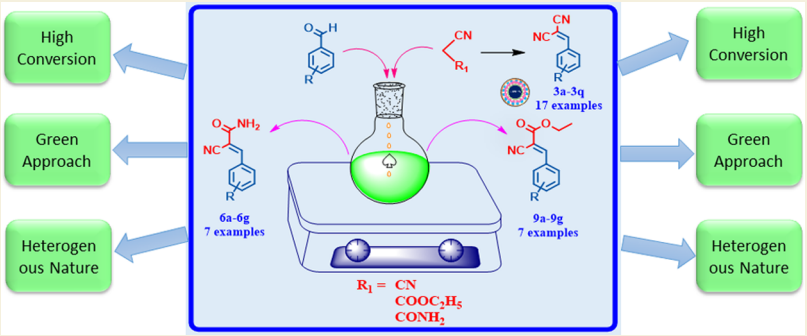

ABSTRACT: Designing efficient, economical heterogeneous catalysts for the Knoevenagel condensation reaction is highly significant owing to the importance of reaction products in industries as well as pharmaceutics. Herein, we have designed and synthesized biguanidine-functionalized basic magnetically retrievable cobalt ferrite nanoparticles (CFNPs) for the synthesis of Knoevenagel condensation products using benzaldehydes and active methylene compounds (malononitrile/ethyl cyanoacetate/cyanoacetamide). Several advanced techniques, such as Fourier transform infrared (FT-IR), thermogravimetric analysis (TGA), powder X-ray diffraction (XRD), scanning electron microscopy (SEM), transmission electron microscopy (TEM), and vibration sample magnetometry (VSM), were utilized to precisely characterize the catalyst. The robust features of the current approach involve outstanding catalytic performance, solvent-free reaction conditions, ease of catalyst retrievability, easy workup procedure, large substrate tolerance, high turnover frequency (TOF) values (up to 486.88 h^{-1}), values of green chemistry metrics such as E-factor (0.15), reaction mass efficiency (RME) value (87.07%), carbon efficiency (93.4%), and atom economy (AE) value (88.10%) close to their ideal values, and recyclability up to eight runs without a considerable reduction in activity, boosting the appeal of this approach from a commercial and ecological point of view.

KEYWORDS: *green approach, magnetic nanocatalyst, reusable, Knoevenagel condensation, solvent-free*

1. INTRODUCTION

The Knoevenagel condensation, a well-known reaction involving aldehydes and activated methylene group-containing molecules, has gained immense significance and widespread adoption as a highly influential and beneficial approach in organic chemistry for the synthesis of C−C bond formation to generate substituted electrophilic alkenes.[1,2] The alkenes thus formed act as versatile intermediates in various organic synthesis applications. These applications encompass a wide range of fields, including the production of fine chemicals, formation of heterocyclic compounds, carbohydrates, and synthesis of drug intermediates, natural products, fluorescent dyes, and functional polymers.[3−8]

Moreover, the applicability of Knoevenagel condensation in various industries such as polymers and pharmaceutical synthesis of various products and intermediates has been well documented.[4] This type of condensation reaction turned out to be a key step for producing numerous clinical drugs.[9] Some of the commercially available drugs involving the Knoevenagel condensation reaction are shown in Figure 1. Besides their enzyme inhibiting properties, the substituted alkene compounds exhibit a vast array of biological studies such as anticancer, antioxidant, antimalarial, antihypertensive, and antiviral properties.[6,10] Furthermore, the Knoevenagel condensation is extensively employed in industries for various

Received: January 23, 2023
Revised: May 30, 2023
Accepted: June 1, 2023
Published: June 23, 2023

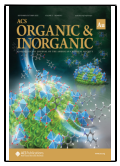

https://doi.org/10.1021/acsorginorgau.3c00002
ACS Org. Inorg. Au 2023, 3, 254−265

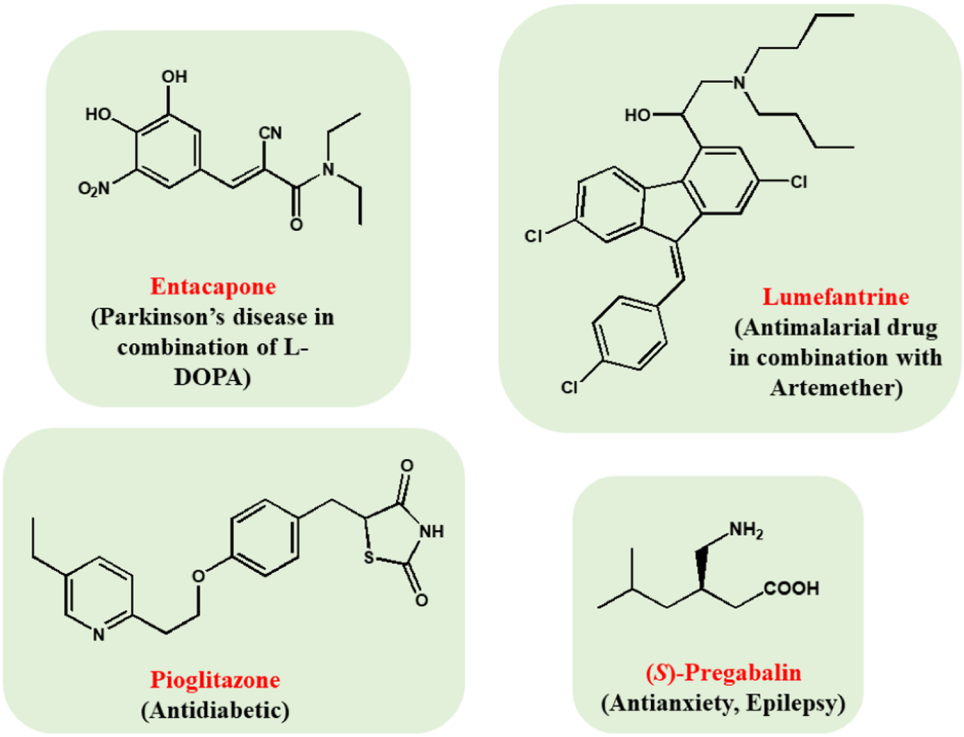

Figure 1. Some of the commercially available drugs derived using the Knoevenagel condensation reaction.

synthetic organic methods as this type of condensation reaction is devoid of any waste and byproducts.[11]

Benzylidenemalononitrile (BMN) derivatives formed by the Knoevenagel condensation involving benzaldehydes and malononitrile also have gained the attention of many research groups owing to their exceptional properties such as anticancer, antifungal, antibacterial, and anticorrosive.[12] The benzylidenemalononitrile derivatives are also used for enhancing cellular resistance to oxidative stress and prostaglandin production, for designing photoconductive cells, and for the activation/inhibition of certain types of enzymes.[13−16]

Taking into consideration the desirability and applicability of these derivatives, there is an urgent need for a simple and employable synthetic procedure for Knoevenagel condensation which is cost-effective as well as energy-saving.

This condensation reaction is frequently carried out using a basic catalyst, as the basic sites present over the catalyst attract protons from the adsorbed active methylene molecules such as malononitrile in order to generate carbanion intermediates. In order to catalyze this Knoevenagel condensation reaction, several homogeneous and heterogeneous (several different types of) catalysts such as zeolites, ionic liquids, Lewis acids, basic catalysts (urea, thiourea, and piperidine), ammonium salts, amino acids, aliphatic amines, metal oxides, metal−organic frameworks (MOFs), carbon materials, graphene-supported Pd and Ni nanoparticles, and covalent organic frameworks (COFs) have been employed.[1,3,5,6,9,11] However, the applicability of these catalysts is limited owing to various environmental issues, such as post-treatment of the generated waste liquid, severe reaction conditions, elevated temperature, use of additives, costly metals, insufficient yields, extensive reaction period, harmful solvents, corrosion of equipment, and tedious workup procedure.[5,11] Also, some of these reported procedures suffer from various other serious problems including the formation of unwanted side products and the production of waste due to self-condensation, addition, and polymerization reactions.[6]

Thus, keeping in mind these restrictions, the aspects of green chemistry, and process sustainability, efforts have been made to develop efficient and reusable heterogeneous catalysts, which can efficiently catalyze this condensation reaction.

Transition metal oxides with the following formula MFe_2O_4, where M = nickel, copper, cobalt, zinc, and manganese, have gained tremendous attention owing to their exceptional physical as well as chemical properties. Among these, cobalt ferrite nanocomposites are a steady magnetic material, which is well-thought-out as the most prominent support due to its substantial magnetic properties such as higher saturation magnetization (Ms) value, relatively high permeability, high intrinsic coercivity, high Curie temperature, biocompatibility, nontoxicity, and chemical stability.[17−20] Several chemical procedures have been developed to synthesize $CoFe_2O_4$ nanoparticles including electrospinning, Co precipitation, sol−gel, sonochemical, combustion, and hydrothermal−solvothermal−hydrothermal methods.[18−20]

These properties have led to their widespread adoption in a wide range of fields, including but not limited to sensors, ferrofluid technology, nanobiotechnology, microwave absorbers, anticancer agent, MRI,[21] biosensors, reduced-toxicity drug delivery, magnetic energy storage, photocatalysis, environmental remediation, catalysis, antimicrobials, and more.[19,20,22−25]

Building on our current protocol to establish synthetic routes that are sustainable for a variety of organic transformations, we have been utilizing a range of advanced materials;[26−29] we have designed this solid biguanidine-functionalized base catalyst (CFNP) as a Lewis basic catalyst having abundant N atoms due to the presence of two imine-like functions over the biguanidine group. The Knoevenagel condensation reaction was studied and used to evaluate the

https://doi.org/10.1021/acsorginorgau.3c00002
ACS Org. Inorg. Au 2023, 3, 254−265

Scheme 1. Pictorial Representation of the Synthesis of the CFNP Nanocatalyst

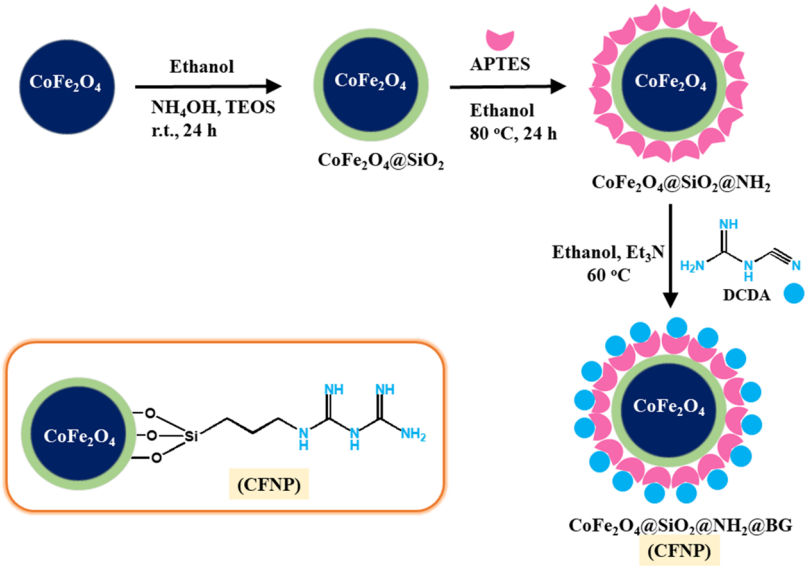

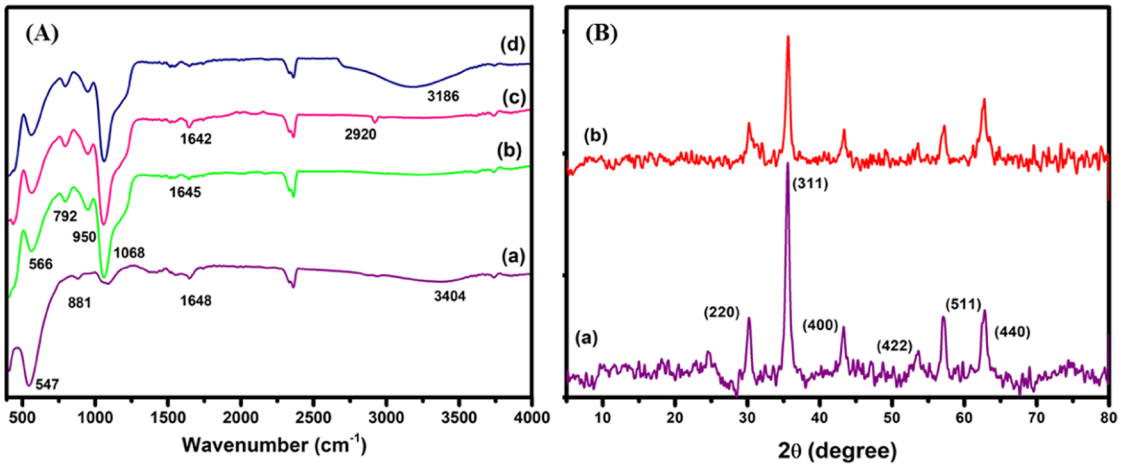

Figure 2. (A) FT-IR spectra of (a) $CoFe_2O_4$, (b) silica-coated $CoFe_2O_4$ ($CoFe_2O_4$@SiO_2), (c) $CoFe_2O_4$@SiO_2@NH_2, and (d) CFNP. (B) Powder XRD analysis of (a) $CoFe_2O_4$ and (b) CFNPs.

more effective material's catalytic activity. This reaction was carried out under solvent-less conditions, lesser reaction time (4−10 min), and high yields.

2. EXPERIMENTAL SECTION

2.1. Catalyst Preparation

2.1.1. Experimental Procedure for the Synthesis of $CoFe_2O_4$. One-pot solvothermal synthesis (Scheme 1)[30] was used to produce magnetic nanoparticles of cobalt ferrite ($CoFe_2O_4$). To make a uniform solution, we added $CoCl_2.6H_2O$ (148 mg, 0.625 mmol) and $FeCl_3.6H_2O$ (337 mg, 1.25 mmol) to 10 mL of ethane-1,2-diol and agitated the mixture constantly at 50 °C. After obtaining a homogenous reaction mixture, 900 mg of NaOAc and 500 mg of PEG-6000 were added and agitated for an additional 30 min. The resulting liquid was transported to an autoclave and heated to 160 °C for 16 h. The resulting black-colored material was separated magnetically and rinsed repeatedly in double-deionized water. Nanoparticles of cobalt ferrite ($CoFe_2O_4$) were produced and dried at 60 °C for 6 h.

2.1.2. Experimental Procedure for the Synthesis of $CoFe_2O_4$@SiO_2. The Stöber sol−gel process was then used to cover the cobalt ferrite nanoparticles ($CoFe_2O_4$) with silica.[28−31] To achieve this, 200 mg of $CoFe_2O4$ nanoparticles (0.852 mmol) was sonicated in 200 mL of a solution made up of 160 mL of EtOH and 40 mL of double-deionized water. Then, 1.5 mL of 25% NH_3 solution and 1 mL of tetraethyl orthosilicate were added dropwise. The resultant dispersed solution was then constantly stirred at 60 °C for 6 h. The final silica-coated nanoparticles were magnetically separated using an external magnet, washed numerous times with ethanol, and then dried under vacuum.

2.1.3. Experimental Procedure for the Synthesis of (CFNA) $CoFe_2O_4$@SiO_2@NH_2. By using our prior method,[29] which included adding 1 mL of (3-aminopropyl)triethoxysilane (APTES) to 0.5 g of $CoFe_2O_4$@SiO_2 nanoparticles dispersed in 100 mL of EtOH, we were able to introduce amine groups onto the surface of silica-coated cobalt ferrite nanoparticles. The final mixture was agitated at 80 °C for 6 h. After that, the synthesized CFNA nanocomposites were collected using an extrinsic magnet, washed with Et_2O to get rid of the silylating agent that had not been reacted, and dried till vacuum.

2.1.4. Synthesis of CFNPs. Biguanidine was added to the surface of the nanocomposite ($CoFe_2O_4$@SiO_2@NH_2) in order to enhance the catalytic sites (NH sites). For this surface modification, 10 mL of EtOH was mixed with 0.5 g of CFNA nanoparticles, 125 mg of dicyandiamide, and 0.3 mL of Et_3N and refluxed for 6 h. The end product, $CoFe_2O_4$@SiO_2@NH_2@BG (CFNP) nanoparticles (Scheme 1), was collected by using an external magnet, washed repeatedly with EtOH, and then dried in an oven for 24 h at 100 °C.

https://doi.org/10.1021/acsorginorgau.3c00002
ACS Org. Inorg. Au 2023, 3, 254−265

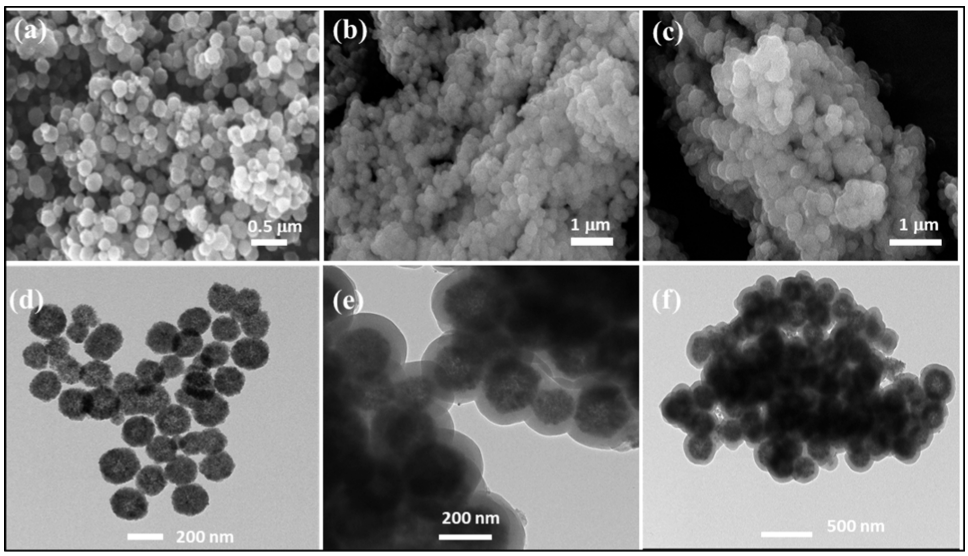

Figure 3. SEM images of (a) $CoFe_2O_4$, (b) $CoFe_2O_4$@SiO_2, and (c) CFNP and TEM images of (d) $CoFe_2O_4$, (e) $CoFe_2O_4$@SiO_2, and (f) CFNP.

2.2. General Procedure for Knoevenagel Condensation Using CFNP as a Catalyst

All the benzaldehydes (1, 4, 7) used during the experiment were purchased from Fluka, Sigma-Aldrich, Merck, Spectrochem, and malononitrile (2), ethyl cyanoacetate (4), and cyanoacetamide (8) were bought from Spectrochem and utilized without undergoing any further purification before being used.

Benzaldehyde (1.0 mmol), an active methylene compound (malononitrile/ethyl cyanoacetate/cyanoacetamide), and 10 mg of the nanocatalyst (CFNP) were placed in a 25 mL oven-dried round-bottom flask. The reaction mixture was stirred constantly at 60 °C. The completion of the condensation process was carefully monitored using TLC with 20% ethyl acetate in hexane as the mobile phase. Ethanol was then added when the reaction was complete, and the catalyst was separated using an external magnet and washed in ethanol. The solvent was evaporated using a rotatory evaporator, and the resultant solid was recrystallized using ethanol.

3. RESULTS AND DISCUSSION

3.1. Catalyst Characterization

To validate the structural attributes of the synthesized nanocatalyst, multiple characterization techniques were used, which are discussed below.

3.1.1. Fourier Transform Infrared (FT-IR) Spectroscopy. FT-IR spectra of $CoFe_2O_4$, $CoFe_2O_4$ @SiO_2, CFNA, and CFNPs were obtained at room temperature using a Perkin Elmer Spectrum 2000 utilizing the KBr pellet method (400−4000 cm^{-1}), as shown in Figure 2A. Absorption bands at 881 and 547 cm^{-1} in the FT-IR spectra of $CoFe_2O_4$ nanoparticles provide evidence for the existence of inverted spinal cobalt ferrite structures.[32] Peaks at 881 and 547 cm^{-1} correspond to the stretching vibration of the tetrahedral site (Fe^{3+}, O^{2-}) and octahedral site (Co^{2+}, O^{2-}) in the spinel structure, respectively. Figure 2A(a) shows the stretching and bending vibrations of the surface OH groups present at 3404 and 1648 cm^{-1}, respectively.[30] In addition, the presence of silica over the surface of cobalt ferrite nanoparticles is confirmed by the bands seen at 792, 950, and 1068 cm^{-1} in Figure 2A(b),[33] which could be attributed to the Si−O−Si symmetric, Si−O symmetric, and Si−O−Si asymmetric stretching modes, respectively. Two additional bands, at 2920 (CH_2) and 1642 (NH_2) cm^{-1}, occur in the spectrum of APTES-functionalized $CoFe_2O_4$@SiO_2 nanoparticles, indicating the surface functionalization of $CoFe_2O_4$@SiO_2 with NH_2 groups (Figure 2A(c)).[34] Furthermore, Figure 2A(d) represents the FT-IR spectra of CFNPs, which are reported earlier.[35] Thus, the findings showed that CFNA nanoparticles were successfully functionalized with the required biguanidine moiety.

3.1.2. XRD Analysis. X-ray diffraction (XRD) was analyzed by the structural integrity and crystalline phase structure of the synthesized $CoFe_2O_4$ and CFNPs. XRD patterns were acquired at room temperature in the 2θ range of 5−80° (Figure 2(B)) using the parameters 0.15406 nm, 40 kV, 40 mA, and scanning rate = 2°/min.

Nanoparticles of inverse cubic spinel cobalt ferrite exhibit characteristic diffraction peaks at 30.24, 35.62, 43.33, 53.60, 57.27, and 62.79°, which correspond to the (220), (311), (400), (422), (511), and (440) planes, respectively, with the space group fd-3m[36] (JCPDS card no. 22-1086, Figure 2B(a)).[28,30] Figure 2B(a) shows that the XRD structure of the sample is consistent with that reported in the previous literature[37] for $CoCl_2.6H_2O$ (JCPDS file (no. 01-0173)), with the exception of a slight shift in the peaks caused by the presence of bimetallic nature (Co and Fe). Additionally, the Bragg diffraction peaks for CFNP were similar and matched with characteristics peaks of cobalt ferrite nanoparticles, confirming that the spinel structure of $CoFe_2O_4$ nanoparticles remains even after chemical transformations (Figure 2B(b)). The XRD pattern showed intense peaks, which is consistent with increased $CoFe_2O_4$ crystallization.

3.1.3. SEM and TEM Analysis. In order to derive information about the shape and morphology of the synthesized nanoparticles ($CoFe_2O_4$, $CoFe_2O_4$@SiO_2, and CFNP), scanning electron microscopy (SEM) images were collected through using a Carl Zeiss, India (Jeol Japan Mode: JSM 6610LV), and transmission electron microscopy (TEM) images of the synthesized nanoparticles were acquired using an FEI TECHNAI (model number G^2 T20) operated at 200 kV by casting their dispersed ethanolic solution over carbon-coated copper grids. The morphology and their texture illustration were attained using scanning electron microscopy and transmission electron microscopy analysis (Figure 3). The SEM pictures collected for $CoFe_2O_4$ nanoparticles substanti-

https://doi.org/10.1021/acsorginorgau.3c00002
ACS Org. Inorg. Au 2023, 3, 254−265

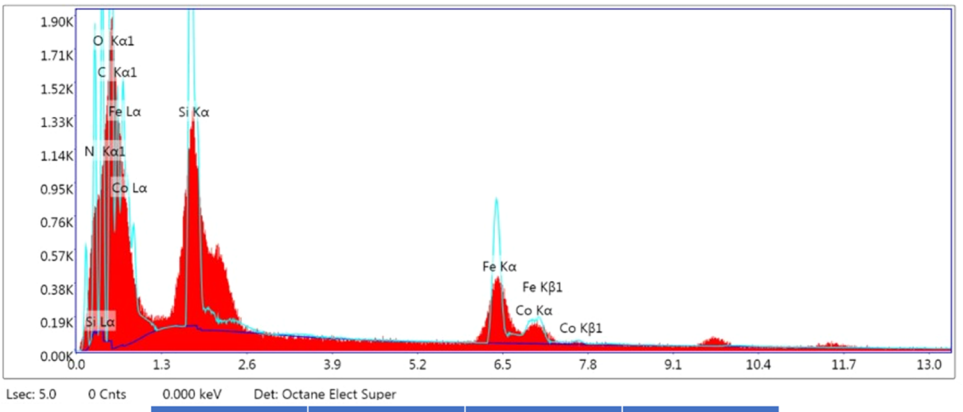

Element	Weight %	Atomic%	Error%
C K	18.54	24.93	8.99
N K	25.27	29.13	9.90
O K	38.61	38.97	9.91
Si K	6.72	3.87	4.24
Fe K	9.40	2.72	3.59
Co K	1.45	0.40	19.01

Figure 4. SEM-coupled EDX spectrum of CFNP.

ated the formation of the monodispersed spherical shape without agglomeration despite the dipolar interaction between the particles.[38] (Figure 3a). The SEM analysis of silica-coated nanoparticles ($CoFe_2O_4$@SiO_2) and after surface modification by the biguanidine group (CFNP) depicted the intactness of their spherical shape (Figure 3b−c). Furthermore, the TEM analysis confirmed that the spherical shape of $CoFe_2O_4$ nanoparticles is monodisperse and the size is about 200 nm (Figure 3d). TEM imaging (Figure 3e) confirms the existence of a uniform silica covering of roughly 30 nm around the $CoFe_2O_4$ core, which prevents agglomeration. The TEM picture of CFNPs further supported the preservation of the same spherical shape and the expanded size of these nanoparticles (Figure 3f). Figure S1b (Supporting information) represents the SAED pattern of $CoFe_2O_4$ nanoparticles, which confirmed the polycrystalline nature of the synthesized nanoparticles due to the existence of diffraction rings with white spots.[39]

Furthermore, to understand the elemental composition of the CFNP nanocatalyst, the SEM-coupled EDX spectrum was collected, and it confirms the presence of expected elements such as cobalt (Co, 1.45%), iron (Fe, 9.40%), silicon (Si, 6.72%), carbon (C, 18.54%), nitrogen (N, 25.27%), and oxygen (O, 38.61%), indicating the successful conjugation of biguanidine with $CoFe_2O_4$@SiO_2@NH_2 nanoparticles (Figure 4).

3.1.4. VSM Analysis. The magnetic properties of the synthesized $CoFe_2O_4$, $CoFe_2O_4$@SiO_2, $CoFe_2O_4$@SiO_2@NH_2, and CFNPs were evaluated using a vibration sample magnetometer (VSM), model number EV-9, Microsense at room temperature (Figure 5). As it can be seen clearly from Figure 5, there is the absence of the hysteresis phenomenon, remanent magnetization, and coercivity, implying the super paramagnetic behavior of bare as well as surface-modified nanoparticles.[40] The values of saturation magnetization (Ms) for $CoFe_2O_4$, silica-coated $CoFe_2O_4$, CFNA, and CFNP were determined to be 63, 53, 48, and 34 emu/g, respectively. The

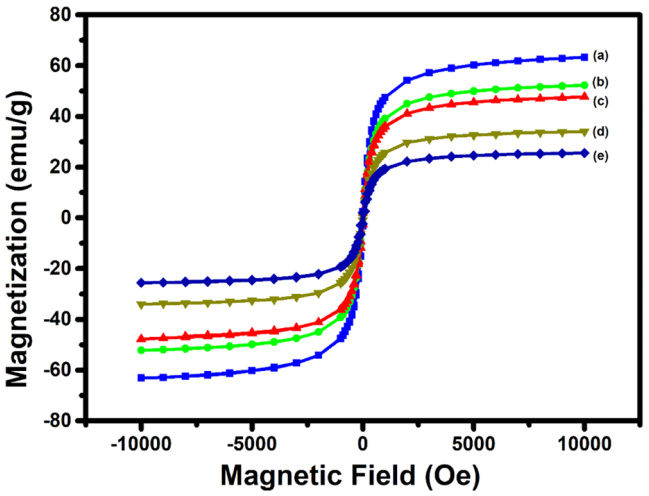

Figure 5. VSM analysis of (a) $CoFe_2O_4$, (b) $CoFe_2O_4$@SiO_2, (c) $CoFe_2O_4$@SiO_2@NH_2, (d) CFNP, and (e) reused CFNP after eight consecutive cycles.

monolayer covering of APTES on the surface caused a very slight drop in the Ms value of $CoFe_2O_4$ after APTES functionalization.[39] This difference in Ms values of $CoFe_2O_4$ and CFNP showed that a great number of biguanidine moieties were bonded to $Co_2Fe_2O_4$ nanoparticles.[32] The addition of nonmagnetic silica and other functional groups may reduce the surface moments for distinct particles, which contributes to the overall drop in magnetism. Despite the lower Ms value for the CFNP in comparison to bare $CoFe_2O_4$, it is still sufficient to perform magnetic separation more quickly from the crude solution by introducing an extrinsic magnetic field. The Ms value for the recovered catalyst was 26 emu/g at rt, which is more than adequate for the efficient and rapid recovery utilizing an external magnet (Figure 5e).

3.1.5. Thermogravimetric Analysis (TGA). Thermogravimetric analysis[26] (TGA) of the sample was carried out on a

https://doi.org/10.1021/acsorginorgau.3c00002
ACS Org. Inorg. Au 2023, 3, 254−265

Shimadzu TG/DTA simultaneous measuring instrument (Model: DTG-60) from ambient temperature (rt) to 800 °C at a steady 10 °C per min heating rate and 100 mL per min nitrogen gas flow to determine the thermal stability of CFNPs. The results indicated that the synthesized CFNPs were stable up to 300 °C in a N_2 environment (Figure 6). Evaporation of

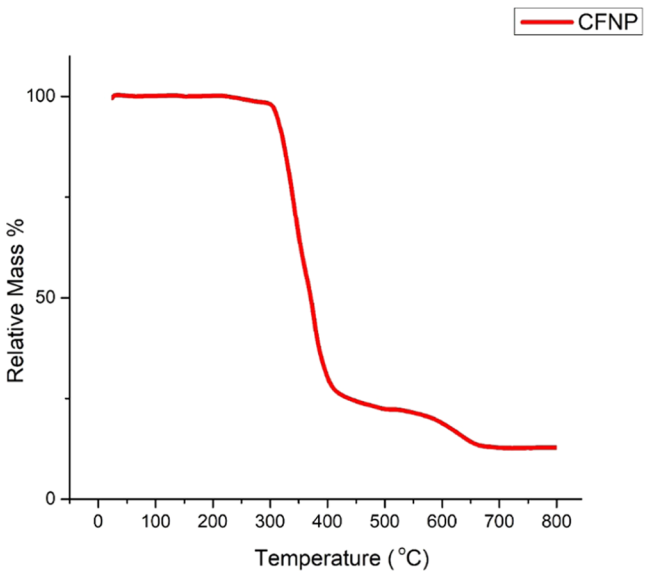

Figure 6. TGA analysis of CFNPs.

the entrapped water and organic solvents causes a minor loss in weight between 230 and 300 °C, but the significant weight loss above 400 °C is due to the disintegration of organic layers. A total weight loss of up to 75% shows that a large portion of the catalyst was composed of organic layers. After 400 °C, the CFNPs start decomposing at 400 °C, which is completed at 650 °C. A further increase in the temperature did not show any decomposition of CFNPs.

3.1.6. Basicity of Catalysis. The quantification of basic sites over the present CFNA and CFNP nanocatalysts was carried out using the conductometric titration method as reported elsewhere.[27] The experimental results showed that the number of basic sites as calculated using conductometric titration was found to be 1.4 mmol/g for CFNA and 3.05 mmol/g for CFNP.

3.1.7. X-ray Crystallographic Structure of Compound 6b. Data were collected using graphite-monochromated Mo Kα radiation (λ = 0.71073 Å) on an XtaLAB Synergy, Dualflex, HyPix3000 diffractometer running at 50 kV and 30 mA. The crystal was analyzed at 293(2) K while the data were being recorded. Using Olex2,[41] the structure was analyzed and refined using the SHELXL[42] refinement package involving least squares minimization. For crystal growth, the Knoevenagel adduct 6b was added in a 50 mL beaker, dissolved in 10 mL of DCM, and kept for few days. The structure analysis of one of the synthesized compound 6b is done by using X-ray single-crystal diffraction (CCDC-2210747, Figure 7). The detailed crystallographic studies of compound 6b[43] $C_{12}H_{10}ClNO_2$ (M = 235.66 g/mol) indicated that the compound has a monoclinic structure in the crystal lattice, space group $P21/n$, and the Z value is 4.

From crystal structure, it is clear that for the given organic molecule 6b and its derivatives, the configuration is E, by using IUPAC convention. Important bond length and bond angle can be seen in Tables S8 and S9, respectively, as mentioned in the Supporting Information.

3.2. Catalytic Potential Analysis of the Biguanidine-Functionalized Cobalt Ferrite Nanocatalyst for the Knoevenagel Condensation

The catalytic potential in the Knoevenagel condensation with benzaldehydes and malononitrile was investigated using the synthesized CFNP nanocatalyst. The reaction conditions were optimized by taking 4-bromobenzaldehyde and malononitrile as test substrates under solvent-free conditions. To accomplish the optimal reaction conditions, effects of the quantity of the catalyst, solvent, temperature, and reaction completion time were studied and optimized (Table 1).

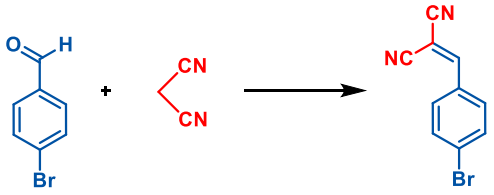

Primarily, the impact of the quantity of the catalyst on the product yield was investigated. The catalytic amount selected for the reaction varies from 0 mg to 15 mg (Table 1, entry 1−4 and 10) at 60 °C, and it was observed that the best results were obtained when 10 mg of CFNP was utilized to perform the reaction (Table 1, entry 4). Using the lower amount of the catalyst, i.e., 5 mg and 7 mg, the yield of the product was found to be less with 70 and 90% yield, respectively (Table 1, entry 2−3), whereas no noticeable change in the isolated yield of the product even after increasing the quantity of the catalyst is observed. When performing the reaction at 60 °C and varying the quantity of the catalyst CFNP from 0 to 15 mg (Table 1, entries 1−4 and 10), it was found that 10 mg of CFNP produced the finest results (Table 1, entry 4). Using a lower quantity of the catalyst, i.e., 5 mg and 7 mg, resulted in a lesser product yield of 70 and 90%, respectively (Table 1, entries 2−3), while increasing the catalyst amount had no noticeable

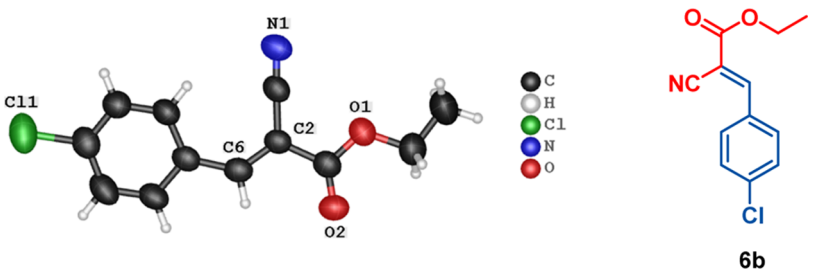

Figure 7. Single-crystal XRD of compound 6b (CCDC- 2210747). The displacement ellipsoid contour is drawn at the 50% probability level.

https://doi.org/10.1021/acsorginorgau.3c00002
ACS Org. Inorg. Au 2023, 3, 254−265

Table 1. Optimization of Reaction Conditions[a]

entry	catalyst amount[b]	solvent	temp (°C)	time[c] (min)	yield (%)[d]
1.	0		60	30	NR
2.	5		60	10	70
3.	7		60	10	90
4.	**10**		**60**	**5**	**99**
5.	10	EtOH	60	10	95
6.	10	DCM	60	10	70
7.	10	CH_3CN	60	10	78
7.	10	THF	60	10	85
8.	10	H_2O	60	10	90
9.	10	toluene	60	10	80
10.	15		60	5	99
11	10		rt	10	72
12.	10		80	5	98
13.	10[e]		40	5	88
14.	10[f]		60	8	88

[a]**Reaction Conditions**: 4-bromobenzaldehyde (1.0 mmol) and malononitrile (1.2 mmol). [b]catalyst (mg). [c]time (min). [d](%) isolated yield. [e]catalyst[27] (ASMNPs),. [f]catalyst (CFNA).

effect on the isolated yield. Therefore, using a catalyst amount of 10 mg yielded the optimum outcomes. Furthermore, on varying the solvents such as EtOH, DCM, CH_3CN, THF, H_2O, and toluene, we did not observe any significant increase in the overall yield of the product (Figure 8, entry 5−9 and Table 1).

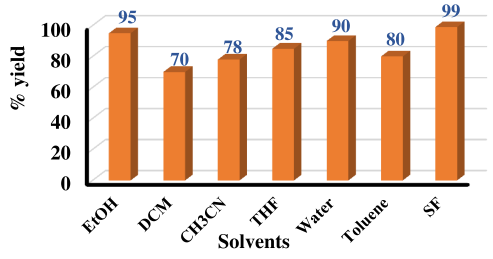

Figure 8. Solvents effect on the yield of the Knoevenagel condensation product [SF corresponds to solvent-free conditions].

Subsequently, the impact of temperature on the reaction's progression was also studied. The yield of the product at rt was found to be 72% only, whereas the increase of temperature from 40 to 60 °C leads to an increase in the isolated yield of the product. One possible explanation for the higher yield is that increasing the temperature also increases the reactant solubility, which ultimately improves the catalytic performance. In addition, neither the pace of the reaction nor the isolated yield of the product was significantly changed by an increase in temperature from 60 to 80 °C (entry 12, Table 1). Along with the present catalyst CFNP, the model reaction was also carried out using our previously reported magnetic basic nanocatalyst (ASMNPs),[27] which is (Fe_3O_4@SiO_2@NH_2), and a noteworthy yield (88%) of the model reaction product was found at 40 °C within 5 min. However, the current magnetic nanocatalyst (CFNP) has a great number of catalytic active sites compared to ASMNPs; the reaction proceeded more efficiently and smoothly. Additionally, we used the catalyst CFNA[f] ($CoFe_2O_4$@SiO_2@NH_2) and CFNP to compare the model reaction's notable yield, which we found to be 88 and 99%, respectively. Considering this, CFNPs show superior catalytic activity compared to CFNA and ASMNPs.

3.2.1. Green Chemistry Parameters. For the synthesis of the Knoevenagel condensation product (3a), the green chemistry metrics for the condensation process between 4-bromobenzaldehyde and malononitrile were also analyzed. Table 2 shows some of the variables considered when analyzing the cost effectiveness of green organic synthesis under ideal circumstances. The radar chart (Figure 9) showed

Table 2. Calculation of Green Chemistry Metrics

yield	atom economy (AE)	reaction mass efficiency (RME)	E-factor	carbon efficiency (CE)
99%	88.10%	87.07%	0.15	93.4%

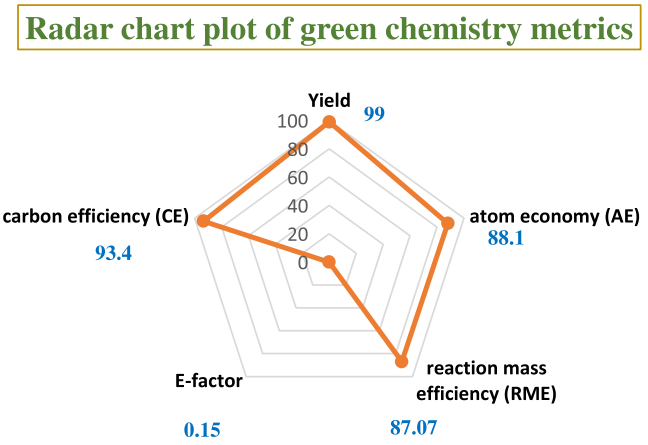

Figure 9. Green chemistry metrics for the synthetic "3a" from a model Knoevenagel condensation process shown on a radar chart plot.

the harmonious relationship between reaction mass efficiency, carbon efficiency, atom economy, and the E-factor, which shows that this approach is environmentally friendly. The supplementary file explains every calculation used to determine green chemistry parameters.

3.3. Knoevenagel Condensation of Aldehydes with an Active Methylene Molecule (Malononitrile, Ethyl Cyanoacetate, or Cyanoacetamide) and the Catalytic Role of CFNPs

After optimizing the reaction conditions for the aforesaid Knoevenagel condensation, the capability of the synthesized nanocatalyst (CFNP) toward the synthesis of the condensation product (benzylidene) was extended and investigated by taking a diverse range of aromatic aldehydes/benzaldehydes and malononitrile (Schemes 2 and 3). Briefly, this condensation reaction was achieved by heating aldehyde (1.0 mmol), malononitrile (1.2 mmol), and the catalyst (10 mg) in an oil bath to 60 °C for a suitable amount of time. Using malononitrile and several aromatic aldehydes containing either electron-withdrawing or electron-donating groups, we were able to generate a wide variety of useful Knoevenagel condensation products in good to great yield, as illustrated in Scheme 2. In addition, the outcomes demonstrated that the electronic environment of the benzylidene utilized affects how quickly benzylidene converts and how much is produced. Electron-withdrawing benzaldehyde derivatives, such as Br, Cl,

https://doi.org/10.1021/acsorginorgau.3c00002
ACS Org. Inorg. Au 2023, 3, 254−265

Scheme 2. Substrate Scope for the Knoevenagel Condensation Involving Aldehydes and Malononitrile using CFNP as a Catalyst[a]

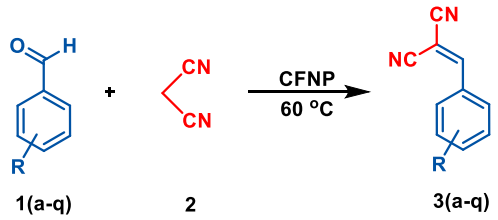

[a]**Reaction Conditions**: Benzaldehyde (1 equiv, 1.0 mmol) and malononitrile (79.27 mg, 0.66 mL, 1.2 equiv, 1.2 mmol), catalyst (10 mg), and temp (60 °C) under neat reaction conditions.

Scheme 3. Substrate Scope for the Knoevenagel Condensation Involving Aldehydes and Ethyl Cyanoacetate using CFNP as a Catalyst[a]

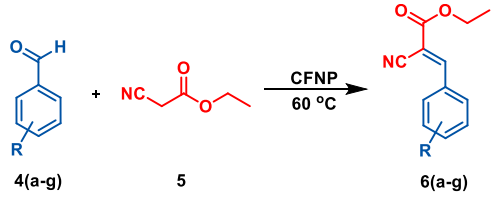

[a]**Reaction Conditions**: Benzaldehyde (1 equiv, 1.0 mmol) and ethyl cyanoacetate (135.7 mg, 1.2 equiv, 1.2 mmol), catalyst (10 mg), and temp (60 °C) under neat reaction conditions

NO_2, CHO, F, and COOH (entry 1a, 1b, 1h, 1l, 1d. 1k), showed superior conversion and better yield as compared to benzaldehydes having electron-donating groups including OMe or CH_3 (entry 1c, 1i).

Additionally, broadening of the use of the Knoevenagel condensation reaction between aldehydes with ethyl cyanoacetate and cyanoacetamide acting as an active methylene compound was also carried out under similar reaction conditions (Schemes 3 and 4). When compared to Scheme 2, it was seen that the reaction proceeds efficiently, which produced an excellent amount of the product.

Scheme 4. Substrate Scope for the Knoevenagel Condensation between Aldehydes and Cyanoacetamide using CFNP as a Catalyst[a]

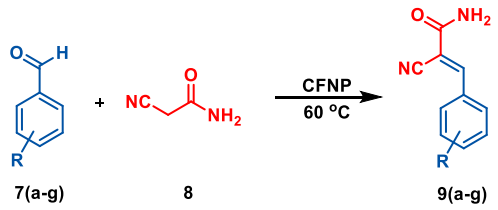

[a]**Reaction Conditions:** Benzaldehyde (1 equiv, 1.0 mmol) and cyanoacetamide (100.89 mg, 1.2 equiv, 1.2 mmol), catalyst (10 mg), and temp (60 °C) under neat reaction conditions.

Additionally, from an industrial perspective, gram-scale synthesis of 2-(4-nitrobenzylidene)malononitrile (3h) was performed. To accomplish this, 1.51 g of *p*-nitrobenzaldehyde (10 mmol), 0.6 mL of malononitrile (12 mmol), and 100 mg of the catalyst CFNP were heated in an oil bath with continuous stirring. After completion of the reaction for compound 3 h, it was found that the reaction proceeded smoothly within 35 min with an excellent yield of 1.49 g (99%). In addition, the current catalytic system was found to be suitable for the conversion involving moderate reaction conditions and an easier workup procedure.

3.4. Probable Reaction Mechanism

A plausible mechanism for the Knoevenagel reaction involving the reactants benzaldehyde and malononitrile using CFNPs as a nanocatalyst for the formation of benzylidene by the condensation method is illustrated in Figure 10. In the beginning, the hydrogen bonds on the catalyst surface were responsible for absorbing the substrates (A). Then, the imine group of the biguanidine moiety (CFNP) abstracts the active α-H of malononitrile and the carbanion formed, which attack the carbonyl carbon of the benzaldehyde to generate an oxyanion (B). After that, the oxyanion thus obtained reacts with the proton of amino cation (C) to form the corresponding Knoevenagel condensation product (benzylidene malononitrile) by removal of a water molecule (D), and the catalyst (CFNPs) is concurrently generated back. Hence, the basic sites of the nanocatalyst played a very vital role in attaining superior performance of the present Knoevenagel condensation reaction.

3.5. Analysis of the Recyclability of the Magnetic Biguanidine-Functionalized Cobalt Ferrite (CFNPs)

Several criteria of green chemistry, including excellent recovery and reusability of the catalyst, are extremely critical and desired features that point in the direction of its commercial implementation. In this regard, 4-bromobenzaldehyde and malononitrile were used as model substrates at the appropriate condensation conditions for the assay of the operational stability and recyclability of the CFNP nanocatalyst. The catalyst was removed magnetically from the reaction mixture when the condensation reaction was complete, washed with ethanol (4−5 times), and then dried at 60 °C under vacuum. After recovering the catalyst, an identical model reaction with benzaldehyde and malononitrile was repeated. The recycling results indicated no appreciable loss in the catalytic activity of the nanocatalyst up to eight consecutive cycles (Figure 11), revealing its exceptional long-term stability and reusability. The CFNP nanocatalyst's activity may have dropped somewhat because the pores were blocked by reactants or products. To further examine the amine group leaching into the reaction mixture, the CFNP was removed from the reaction medium after 3 min using an extrinsic magnet. Now, the residual reaction mixture was reacted under similar circumstances, and no further progress in the reaction was observed even after 40 min, which confirmed the heterogeneous nature as well as stability of the CFNP nanocatalyst. The obtained outcomes were further supported by the FT-IR, powder XRD, and SEM analyses of the recovered catalyst (obtained after the 8th run in the Supporting Information (SI)) and VSM analyses of the recovered catalyst (Figure 5e). The basic nanocatalyst's structure and shape remained unaltered even after eight runs, proving its stability and durability, when the findings of fresh and recovered catalysts were compared.

3.6. Comparison of the CFNP-Catalyzed Knoevenagel Condensation to Form Benzylidenemalononitrile Derivatives with the Reported Precedents

Numerous homogeneous and heterogeneous catalysts have been identified for the Knoevenagel condensation reaction

https://doi.org/10.1021/acsorginorgau.3c00002
ACS Org. Inorg. Au 2023, 3, 254−265

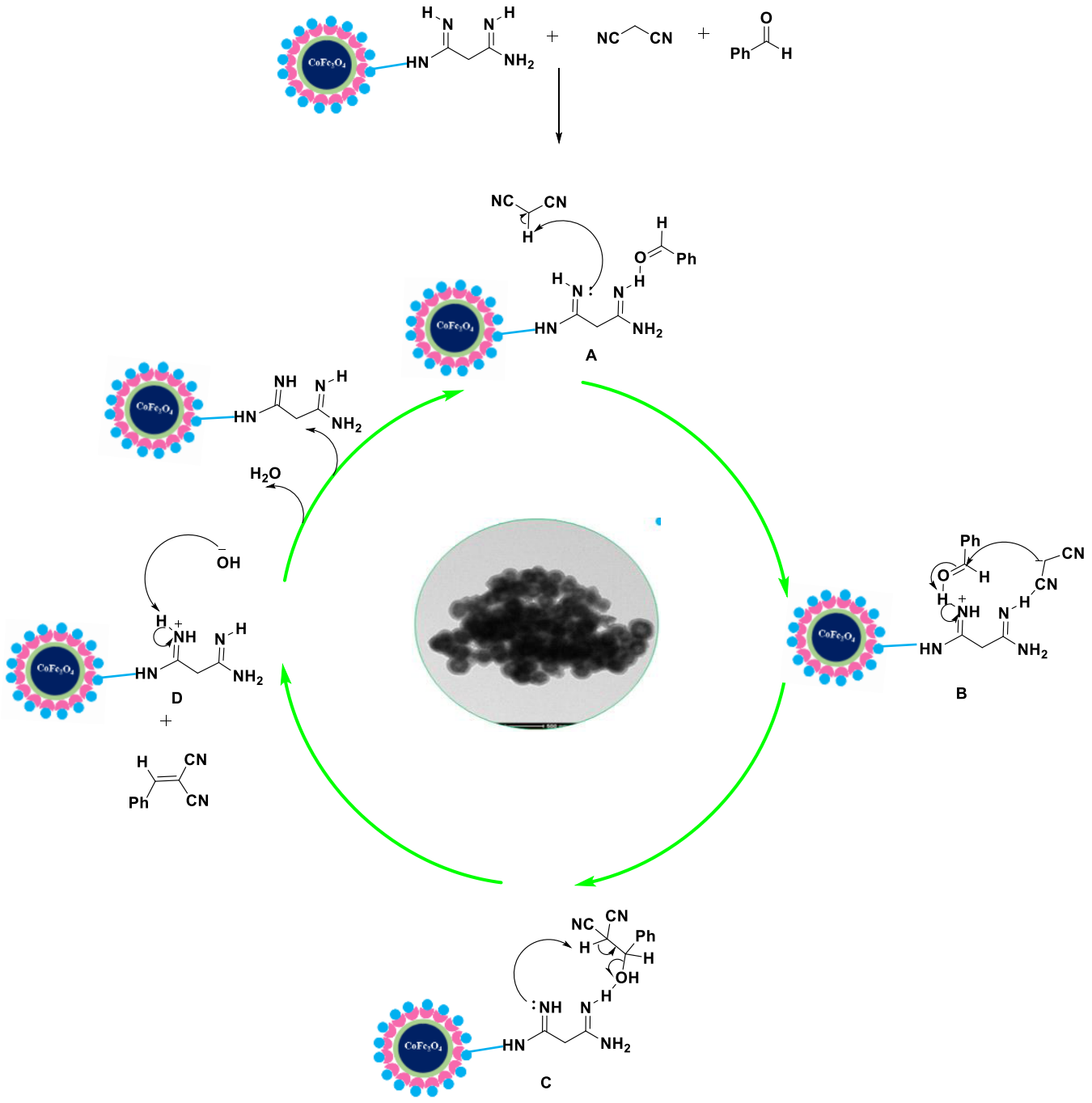

Figure 10. Plausible reaction mechanism for the Knoevenagel condensation reaction involving aldehydes and malononitrile using a basic CFNP nanocatalyst.[44]

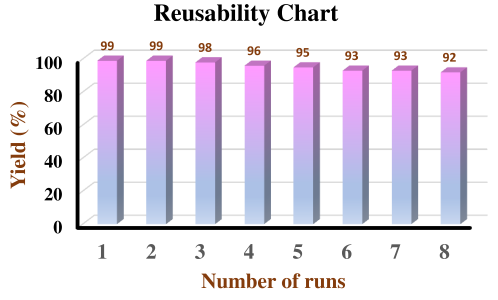

Figure 11. Recyclability chart of the synthesized CFNP catalyst.

involving aldehydes and malononitrile, according to a thorough literature review (Table 3). Our magnetic solid heterogeneous CFNP nanocatalyst outperformed previous reports in ambient reaction conditions, catalyst loading, solvent-free conditions, time, product yield, no need for column chromatography, wide functional group tolerance, catalyst magnetic retrievability, and recyclability. The current magnetic nanocatalyst performs well because it has several basic catalytic sites that support condensation product formation. Thus, the current catalytic system offers a clean and green method without a reaction solvent, simple workup, recyclability, and stability of the biguanidine-functionalized nanocatalyst by applying an external magnetic force.

https://doi.org/10.1021/acsorginorgau.3c00002
ACS Org. Inorg. Au 2023, 3, 254−265

Table 3. Previously Reported Methods and Catalyst for the Knoevenagel Condensation Reaction

s. no.	catalyst	solvent	temp. (°C)	time	yield (%)	refs
1.	NiCu@MW CNT NPs	H_2O/MeOH (1:1)	rt	10−180 min	96	12
2.	FeNPs/PPD@rGO	toluene	40	3.5 h	100	5
3.	$Ce_{0.4}Bi_{0.6}O_{1.7}$	EtOH	35	6h	100	45
4.	Fe_3O_4@CFR-S-PNIPAM@ Pd/CD	H_2O	25	24 h	98	46
5.	GO-NH_2(1.8)−Si (0.2)	H_2O	40	1 h	99	47
6.	PS−NH_2 HMOPBs	EtOH	rt	2 h	98	48
7.	Cu-based MOF	toluene	100	10 h	99	49
8.	$Ga_4B_2O_9$	N_2/DMSO	40	0.5 h	98	9
9.	Fe_3O_4/SiO_2/PPI-G_3	N_2/EtOH	rt	0.5 h	93	50
10.	[CaZn] NUC-21		60	1 h	97	51
11.	UiO-67-diamine	DMF	25	2 h	99	52
12.	(NUC-42)	H_2O	60	6 h	99	53
13.	CFNP	solvent-free	60	5−20 min	99	P.W.

4. CONCLUSIONS

In conclusion, a novel biguanidine-functionalized basic magnetic cobalt ferrite nanocatalyst (CFNP) for the Knoevenagel condensation reaction involving aldehydes and an active methylene compound (malononitrile/ethyl cyanoacetate/cyanoacetamide) has been designed, characterized, and examined for its performance. The current approach's notable features are its superiority over the conventional magnetic core-based nanocatalyst reported previously, which include ambient reaction conditions, the heterogeneous nature of the catalyst, a shorter reaction period (4−30 min), low catalyst loading, a broad substrate scope, high conversion, high TOF values (52.46−486.88 h^{-1}), and high yield of condensation products. The produced nanocatalyst also showed recyclability up to eight successive runs without any notable reduction in its activity, and its removal from the reaction mixture is as easy as using magnetic attraction. In addition, the proposed protocol is green and sustainable to easily synthesize the Knoevenagel condensation products, with use of nonhazardous chemicals, cost effectiveness, solvent-free settings, and a straightforward workup process. We believe that the developed nanocatalyst can find a wide variety of industrial applications for significant organic transformation reactions under green and sustainable conditions due to the presence of a large number of NH groups, which is enabled by the immobilization of a wide variety of chemical and metal moieties.

■ ASSOCIATED CONTENT

Data Availability Statement

The data supporting the findings of this study are available in the published article and its accompanying Supporting Information.

Supporting Information

The Supporting Information is available free of charge at https://pubs.acs.org/doi/10.1021/acsorginorgau.3c00002.

Materials and reagents, instrumentation, green chemistry parameters, TOF calculations, EDX and SAED spectrum of $CoFe_2O_4$, SEM, powder XRD, and FT-IR of the reused catalyst after eight runs, FTIR, ^1H, and ^{13}C NMR shift value, HRMS/elemental analysis, ^1H and ^{13}C NMR spectra of the synthesized compounds, and single-crystal XRD data for compound 6b and references (PDF).

Accession Codes

CCDC 2210747 contains the supplementary crystallographic data for this paper. These data can be obtained free of charge via www.ccdc.cam.ac.uk/data_request/cif, or by emailing data_request@ccdc.cam.ac.uk, or by contacting The Cambridge Crystallographic Data Centre, 12 Union Road, Cambridge CB2 1EZ, UK; fax: +44 1223 336033.

■ AUTHOR INFORMATION

Corresponding Author

Satish K. Awasthi − *Chemical Biology Laboratory, Department of Chemistry, University of Delhi, Delhi 110007, India;* orcid.org/0000-0002-1105-1431; Phone: +91-9582087608; Email: satishpna@gmail.com

Authors

Anupam Mishra − *Chemical Biology Laboratory, Department of Chemistry, University of Delhi, Delhi 110007, India*

Priyanka Yadav − *Chemical Biology Laboratory, Department of Chemistry, University of Delhi, Delhi 110007, India*

Complete contact information is available at: https://pubs.acs.org/10.1021/acsorginorgau.3c00002

Author Contributions

$A.M. and P.Y. contributed equally in this manuscript. CRediT: **Anupam Mishra** data curation (equal), formal analysis (equal), investigation (equal), methodology (equal), project administration (equal), resources (equal), software (equal), writing-review & editing (equal); **Priyanka Yadav** writing-original draft (equal); **Satish Kumar Awasthi** conceptualization (equal), supervision (equal), visualization (equal).

Notes

The authors declare no competing financial interest.

■ ACKNOWLEDGMENTS

A.M. thanks the Department of Science and Technology (DST INSPIRE) for providing a Senior Research Fellowship. P.Y. expresses gratitude to the UGC for the Senior Research Fellowship. S.K.A. acknowledges the financial support received from the University of Delhi, Delhi 110007, India.

REFERENCES

(1) Taher, A.; Lumbiny, B. J.; Lee, I.-M. A facile microwave-assisted Knoevenagel condensation of various aldehydes an d ketones using amine-functionalized metal organic frameworks. *Inorg. Chem. Commun.* **2020**, *119*, No. 108092.

(2) Varnaseri, N.; Rouhani, F.; Ramazani, A.; Morsali, A. Size and function influence study on enhanced catalytic performance of a cooperative MOF for mild, green and fast C−C bond formation. *Dalton Trans.* **2020**, *49*, 3234−3242.

(3) Joharian, M.; Morsali, A.; Tehrani, A. A.; Carlucci, L.; Proserpio, D. M. Water-stable fluorinated metal−organic frameworks (F-MOFs) with hydrophobic properties as efficient and highly active heterogeneous catalysts in aqueous solution. *Green Chem.* **2018**, *20*, 5336−5345.

(4) Li, C.; Zhong, D.; Huang, X.; Shen, G.; Li, Q.; Du, J.; Li, Q.; Wang, S.; Li, J.; Dou, J. Two organic−inorganic hybrid polyoxovanadates as reusable catalysts for Knoevenagel condensation. *New J. Chem.* **2019**, *43*, 5813−5819.

(5) Patel, D.; Vithalani, R.; Modi, C. K. Highly efficient FeNP-embedded hybrid bifunctional reduced graphene oxide for Knoevenagel condensation with active methylene compounds. *New J. Chem.* **2020**, *44*, 2868−2881.

(6) Jain, K.; Chaudhuri, S.; Pal, K.; Das, K. The Knoevenagel condensation using quinine as an organocatalyst under solvent-free conditions. *New J. Chem.* **2019**, *43*, 1299−1304.

(7) Zare, E.; Rafiee, Z. Cellulose stabilized Fe_3O_4 and carboxylate-imidazole and Co-based MOF growth as an exceptional catalyst for the Knoevenagel reaction. *Appl. Organomet. Chem.* **2020**, *34*, No. e5516.

(8) Kalantari, F.; Rezayati, S.; Ramazani, A.; Aghahosseini, H.; Ślepokura, K.; Lis, T. Proline-Cu Complex Based 1, 3, 5-Triazine Coated on Fe_3O_4 Magnetic Nanoparticles: A Nanocatalyst for the Knoevenagel Condensation of Aldehyde with Malononitrile. *ACS Appl. Nano Mater.* **2022**, *5*, 1783−1797.

(9) Yang, Y.; Wang, D.; Jiang, P.; Gao, W.; Cong, R.; Yang, T. Structure-induced Lewis-base $Ga_4B_2O_9$ and its superior performance in Knoevenagel condensation reaction. *Mol. Catal.* **2020**, *490*, No. 110914.

(10) Wu, J.; Hua, W.; Yue, Y.; Gao, Z. A Highly Efficient Bifunctional Catalyst CoO_x/tri-g-C_3N_4 for One-Pot Aerobic Oxidation−Knoevenagel Condensation Reaction. *Catalysts* **2020**, *10*, 712.

(11) Miao, Z.; Yang, F.; Luan, Y.; Shu, X.; Ramella, D. Synthesis of Fe_3O_4@ P4VP@ ZIF-8 core-shell microspheres and their application in a knoevenagel condensation reaction. *J. Solid State Chem.* **2017**, *256*, 27−32.

(12) Zengin, N.; Burhan, H.; Şavk, A.; Göksu, H.; Şen, F. Synthesis of benzylidenemalononitrile by Knoevenagel condensation through monodisperse carbon nanotube-based NiCu nanohybrids. *Sci. Rep.* **2020**, *10*, No. 12758.

(13) Turpaev, K.; Ermolenko, M.; Cresteil, T.; Drapier, J. C. Benzylidenemalononitrile compounds as activators of cell resistance to oxidative stress and modulators of multiple signaling pathways. A structure−activity relationship study. *Biochem. Pharmacol.* **2011**, *82*, 535−547.

(14) Michel, F.; Mercklein, L.; de Paulet, A. C.; Dore, J. C.; Gilbert, J.; Miquel, J. The effect of various acrylonitriles and related compounds on prostaglandin biosynthesis. *Prostaglandins* **1984**, *27*, 69−84.

(15) Shahid, M.; Misra, A. A simple and sensitive intramolecular charge transfer fluorescent probe to detect CN− in aqueous media and living cells. *Anal. Methods* **2013**, *5*, 434−437.

(16) Levitzki, A.; Mishani, E. Tyrphostins and other tyrosine kinase inhibitors. *Annu. Rev. Biochem.* **2006**, *75*, 93−109.

(17) Hedayatnasab, Z.; Abnisa, F.; Daud, W. M. A. W. Review on magnetic nanoparticles for magnetic nanofluid hyperthermia application. *Mater. Des.* **2017**, *123*, 174−196.

(18) Gharibshahian, M.; Mirzaee, O.; Nourbakhsh, M. Evaluation of superparamagnetic and biocompatible properties of mesoporous silica coated cobalt ferrite nanoparticles synthesized via microwave modified Pechini method. *J. Magn. Magn. Mater.* **2017**, *425*, 48−56.

(19) Senthil, V.; Gajendiran, J.; Raj, S. G.; Shanmugavel, T.; Kumar, G. R.; Reddy, C. P. Study of structural and magnetic properties of cobalt ferrite ($CoFe_2O_4$) nanostructures. *Chem. Phys. Lett.* **2018**, *695*, 19−23.

(20) Taghavi Fardood, S.; Moradnia, F.; Mostafaei, M.; Afshari, Z.; Faramarzi, V.; Ganjkhanlu, S. Biosynthesis of $MgFe_2O_4$ magnetic nanoparticles and its application in photo-degradation of malachite green dye and kinetic study. *Nanochem. Res.* **2019**, *4*, 86−93.

(21) Aguiar, A.; Michels, L.; da Silva, F.; Kern, C.; Gomide, G.; Ferreira, C.; Depeyrot, J.; Aquino, R.; da Silva, G. The use of a laponite dispersion to increase the hydrophilicity of cobalt-ferrite magnetic nanoparticles. *Appl. Clay Sci.* **2020**, *193*, No. 105663.

(22) Sorbiun, M.; Shayegan Mehr, E.; Ramazani, A.; Mashhadi Malekzadeh, A. Biosynthesis of metallic nanoparticles using plant extracts and evaluation of their antibacterial properties. *Nanochem. Res.* **2018**, *3*, 1−16.

(23) Kalam, A.; Al-Sehemi, A. G.; Assiri, M.; Du, G.; Ahmad, T.; Ahmad, I.; Pannipara, M. Modified solvothermal synthesis of cobalt ferrite ($CoFe_2O_4$) magnetic nanoparticles photocatalysts for degradation of methylene blue with H_2O_2/visible light. *Results Phys.* **2018**, *8*, 1046−1053.

(24) Chandekar, K. V.; Shkir, M.; Alshahrani, T.; Ibrahim, E. H.; Kilany, M.; Ahmad, Z.; Manthrammel, M. A.; AlFaify, S.; Kateb, B.; Kaushik, A. One-spot fabrication and in-vivo toxicity evaluation of core-shell magnetic nanoparticles. *Mater. Sci. Eng. C* **2021**, *122*, No. 111898.

(25) Zhang, H.; Wang, J.; Zeng, Y.; Wang, G.; Han, S.; Yang, Z.; Li, B.; Wang, X.; Gao, J.; Zheng, L.; et al. Leucine-coated cobalt ferrite nanoparticles: Synthesis, characterization and potential biomedical applications for drug delivery. *Phys. Lett. A* **2020**, *384*, No. 126600.

(26) Mittal, R.; Awasthi, S. K. Bimetallic Oxide Catalyst for the Dehydrogenative Oxidation Reaction of Alcohols: Practical Application in the Synthesis of Value-Added Chemicals. *ACS Sustainable Chem. Eng.* **2022**, *10*, 1702−1713.

(27) Singh, P.; Yadav, P.; Mishra, A.; Awasthi, S. K. Green and mechanochemical one-pot multicomponent synthesis of bioactive 2-amino-4 H-benzo [b] pyrans via highly efficient amine-functionalized SiO_2@ Fe_3O_4 nanoparticles. *ACS Omega* **2020**, *5*, 4223−4232.

(28) Yadav, P.; Kakati, P.; Singh, P.; Awasthi, S. K. Application of sulfonic acid fabricated cobalt ferrite nanoparticles as effective magnetic nanocatalyst for green and facile synthesis of benzimidazoles. *Appl. Catal., A* **2021**, *612*, No. 118005.

(29) Yadav, P.; Awasthi, S. K. Probing the catalytic activity of highly efficient sulfonic acid fabricated cobalt ferrite magnetic nanoparticles for the clean and scalable synthesis of dihydro, spiro and bis quinazolinones. *New J. Chem.* **2021**, *45*, 15928−15941.

(30) Sharma, R. K.; Yadav, S.; Sharma, S.; Dutta, S.; Sharma, A. Expanding the horizon of multicomponent oxidative coupling reaction via the design of a unique, 3D copper isophthalate MOF-based catalyst decorated with mixed spinel $CoFe_2O_4$ nanoparticles. *ACS Omega* **2018**, *3*, 15100−15111.

(31) Rezayati, S.; Kalantari, F.; Ramazani, A.; Sajjadifar, S.; Aghahosseini, H.; Rezaei, A. Magnetic Silica-Coated Picolylamine Copper Complex [Fe_3O_4@ SiO_2@ GP/Picolylamine-Cu (II)]-Catalyzed Biginelli Annulation Reaction. *Inorg. Chem.* **2022**, *61*, 992−1010.

(32) Altun, S.; Çakıroğlu, B.; Özacar, M.; Özacar, M. A facile and effective immobilization of glucose oxidase on tannic acid modified $CoFe_2O_4$ magnetic nanoparticles. *Colloids Surf., B* **2015**, *136*, 963−970.

(33) Ren, C.; Ding, X.; Fu, H.; Li, W.; Wu, H.; Yang, H. Core−shell superparamagnetic monodisperse nanospheres based on amino-functionalized $CoFe_2O_4$@ SiO_2 for removal of heavy metals from aqueous solutions. *RSC Adv.* **2017**, *7*, 6911−6921.

(34) Donia, A. M.; Atia, A. A.; Al-Amrani, W. A.; El-Nahas, A. M. Effect of structural properties of acid dyes on their adsorption

https://doi.org/10.1021/acsorginorgau.3c00002
ACS Org. Inorg. Au 2023, 3, 254−265

behaviour from aqueous solutions by amine modified silica. *J. Hazard. Mater.* **2009**, *161*, 1544−1550.
(35) Niknam, E.; Moaddeli, A.; Khalafi-Nezhad, A. Palladium anchored on guanidine-terminated magnetic dendrimer (G3-Gu-Pd): An efficient nano-sized catalyst for phosphorous-free Mizoroki-Heck and copper-free Sonogashira couplings in water. *J. Organomet. Chem.* **2020**, *923*, No. 121369.
(36) Malinowska, I.; Ryżyńska, Z.; Mrotek, E.; Klimczuk, T.; Zielińska-Jurek, A. Synthesis of $CoFe_2O_4$ nanoparticles: the effect of ionic strength, concentration, and precursor type on morphology and magnetic properties. *J. Nanomater.* **2020**, *2020*, 1−12.
(37) Datta, S.; Mahapatra, A.; Sett, P.; Ghosh, M.; Mallick, P.; Chakrabarti, P. Magnetic measurements, Raman and infrared spectra of metal−ligand complex derived from $CoCl_2{\cdot}6H_2O$ and 2-benzoyl pyridine. *Bull. Mater. Sci.* **2018**, *41*, 1−10.
(38) Agouriane, E.; Rabi, B.; Essoumhi, A.; Razouk, A.; Sahlaoui, M.; Costa, B.; Sajieddine, M. Structural and magnetic properties of $CuFe_2O_4$ ferrite nanoparticles synthesized by co-precipitation. *J. Mater. Environ. Sci* **2016**, *7*, 4116−4120.
(39) Karade, V. C.; Sharma, A.; Dhavale, R. P.; Shingte, S. R.; Patil, P. S.; Kim, J. H.; Zahn, D. R. T.; Chougale, A. D.; Salvan, G.; Patil, P. APTES monolayer coverage on self-assembled magnetic nanospheres for controlled release of anticancer drug Nintedanib. *Sci. Rep.* **2021**, *11*, No. 5674.
(40) Xie, W.; Zhang, C. Production of medium-chain structured lipids using dual acidic ionic liquids supported on Fe_3O_4@ SiO_2 composites as magnetically recyclable catalysts. *LWT* **2018**, *93*, 71−78.
(41) Dolomanov, O. V.; Bourhis, L. J.; Gildea, R. J.; Howard, J. A.; Puschmann, H. OLEX2: a complete structure solution, refinement and analysis program. *J. Appl. Crystallogr.* **2009**, *42*, 339−341.
(42) Sheldrick, G. XS. version 2013/1, Georg-August-Universität Göttingen, Germany, 2013; b) GM Sheldrick. *Acta Crystallogr., Sect. A* **2015**, *71*, 3−8.
(43) Zhang, Y.; Liu, J.-W. Ethyl 3-(4-chlorophenyl)-2-cyanoacrylate. *Acta Crystallogr., Sect. E: Struct. Rep. Online* **2006**, *62*, o5286−o5287.
(44) Yuan, X.; Wang, Z.; Zhang, Q.; Luo, J. An intramolecular relay catalysis strategy for Knoevenagel condensation and 1, 3-dipolar cycloaddition domino reactions. *RSC Adv.* **2019**, *9*, 23614−23621.
(45) Varga, G.; Kukovecz, Á.; Kónya, Z.; Sipos, P.; Pálinkó, I. Green and selective toluene oxidation−Knoevenagel-condensation domino reaction over Ce-and Bi-based CeBi mixed oxide mixtures. *J. Catal.* **2020**, *381*, 308−315.
(46) Yang, Y.; Zhu, W.; Shi, B.; Lü, C. Construction of a thermo-responsive polymer brush decorated Fe_3O_4@ catechol-formaldehyde resin core−shell nanosphere stabilized carbon dots/PdNP nanohybrid and its application as an efficient catalyst. *J. Mater. Chem. A* **2020**, *8*, 4017−4029.
(47) Qian, B.; Wang, F.; Li, D.; Li, Y.; Zhang, B.; Zhu, J. Preparation of a Pickering emulsion by modification of an amine-functionalized graphene oxide surface with organosilane: efficient catalyst for the Knoevenagel condensation of malononitrile with aldehydes at mild temperature. *New J. Chem.* **2020**, *44*, 5995−6002.
(48) Zhang, L.; Zhang, J.; Wei, S.; Li, S.; Ma, X. Amine-functionalized hollow mesoporous nano-bowl with bulky acid-imprinted free space around base sites and DMF-annealed mesoporous channels as an efficient solid base catalyst. *Appl. Catal., A* **2020**, *600*, No. 117560.
(49) Jin, F. An excellently stable heterovalent copper−organic framework based on Cu4I4 and Cu (COO) $2N_2$ SBUs: The catalytic performance for CO_2 cycloaddition reaction and Knoevenagel condensation reaction. *Inorg. Chem. Commun.* **2020**, *116*, No. 107940.
(50) Kannappan, L.; Rajmohan, R. Synthesis of structurally enhanced magnetite cored poly (propyleneimine) dendrimer nano-hybrid material and evaluation of its functionality in sustainable catalysis of condensation reactions. *React. Funct. Polym.* **2020**, *152*, No. 104579.
(51) Chen, H.; Fan, L.; Zhang, X. Highly Robust 3s−3d {CaZn}−Organic Framework for Excellent Catalytic Performance on Chemical Fixation of CO_2 and Knoevenagel Condensation Reaction. *ACS Appl. Mater. Interfaces* **2020**, *12*, 54884−54892.
(52) Xi, F.-G.; Liu, H.; Yang, N.-N.; Gao, E.-Q. Aldehyde-tagged zirconium metal−organic frameworks: a versatile platform for postsynthetic modification. *Inorg. Chem.* **2016**, *55*, 4701−4703.
(53) Chen, H.; Zhang, Z.; Hu, T.; Zhang, X. Nanochannel {InZn}−Organic framework with a high catalytic performance on CO_2 chemical fixation and Deacetalization−Knoevenagel condensation. *Inorg. Chem.* **2021**, *60*, 16429−16438.

https://doi.org/10.1021/acsorginorgau.3c00002
ACS Org. Inorg. Au 2023, 3, 254−265